Molecular and Cellular Neuroscience 59 (2014) 97–105

Contents lists available at ScienceDirect

Molecular and Cellular Neuroscience

journal homepage: www.elsevier.com/locate/ymcne

cJun promotes CNS axon growth

Jessica K. Lerch [a,b,d], Yania R. Martínez-Ondaro [b], John L. Bixby [b,c,*], Vance P. Lemmon [b,**]

[a] Department of Neuroscience, Center for Brain and Spinal Cord Repair, The Ohio State University Wexner Medical Center, 460 W 12th Ave, Columbus, OH 43210, USA
[b] The Miami Project to Cure Paralysis, Department of Neurological Surgery, Miller School of Medicine, University of Miami, 1400 NW 12th Ave, Miami, FL 33136, USA
[c] Department of Molecular and Cellular Pharmacology, Miller School of Medicine, University of Miami, 1400 NW 12th Ave, Miami, FL 33136, USA
[d] University of Miami, Miami, FL, 33136, USA

ARTICLE INFO

Article history:
Received 13 May 2013
Revised 9 January 2014
Accepted 1 February 2014
Available online 9 February 2014

Keywords:
cJun
Axon
Cortical neuron
Regeneration
Transcription factor

ABSTRACT

A number of genes regulate regeneration of peripheral axons, but their ability to drive axon growth and regeneration in the central nervous system (CNS) remains largely untested. To address this question we overexpressed eight transcription factors and one small GTPase alone and in pairwise combinations to test whether combinatorial overexpression would have a synergistic impact on CNS neuron neurite growth. The Jun oncogene/signal transducer and activator of transcription 6 (JUN/STAT6) combination increased neurite growth in dissociated cortical neurons and in injured cortical slices. In injured cortical slices, JUN overexpression increased axon growth to a similar extent as JUN and STAT6 together. Interestingly, JUN overexpression was not associated with increased growth associated protein 43 (GAP43) or integrin alpha 7 (ITGA7) expression, though these are predicted transcriptional targets. This study demonstrates that JUN overexpression in cortical neurons stimulates axon growth, but does so independently of changes in expression of genes thought to be critical for JUNs effects on axon growth. We conclude that JUN activity underlies this CNS axonal growth response, and that it is mechanistically distinct from peripheral regeneration responses, in which increases in JUN expression coincide with increases in GAP43 expression.

Introduction

A multitude of factors contributes to the failure of the CNS to recover after an insult, whether it is disease or injury related. The cellular environment is antagonistic to regeneration because of the formation of a glial and fibrotic barrier (Davies et al., 1999; Tom et al., 2004), immune responses, which generally are prohibitive (Horn et al., 2008; Kigerl et al., 2009), and the inhibitory nature of myelin debris from damaged axons (GrandPre et al., 2000; Lee et al., 2010; Schwab and Caroni, 1988). Even when inhibitory environmental factors are neutralized, adult CNS neurons do not express the appropriate panel of genes to regenerate an axon (Blackmore and Letourneau, 2006; Chen et al., 1995; Goldberg et al., 2002). However, modifying the intrinsic regeneration capacity of injured CNS neurons has been successful. Genetic deletion of phosphatase and tensin homologue (PTEN; Liu et al., 2010; Park et al., 2008), suppressor of cytokine signaling 3 (SOCS3; Smith et al., 2009) or Krüppel-like transcription factor 4 (KLF4; Moore et al., 2009) are examples of how the removal of inhibitory genetic factors promotes regeneration, while in the case of activated KLF7, adding back an axonal growth promoter can enhance regeneration (Blackmore et al., 2012). It seems highly likely that additional transcription factors remain to be identified that contribute to the regeneration process.

PTEN (Park et al., 2008) and KLFs 4/7 (Blackmore et al., 2010; Moore et al., 2009) were identified in screens examining genes associated with cellular proliferation and developmental regulation of axon growth. We implicated signal transducer and activator of transcription 3 (STAT3) as a key regulator of axon growth in dorsal root ganglion (DRG) neurons after comparing gene expression in regenerating peripheral neurons (DRGs) and non-regenerating CNS neurons (cerebellar granular neurons, CGNs; Smith et al., 2011), an observation that has since gained additional support (Bareyre et al., 2011). Our previous studies targeted single genes (Blackmore et al., 2010; Smith et al., 2011) mostly due to technical challenges associated with overexpressing multiple genes. We recently overcame this hurdle and have successfully employed a technique to overexpress multiple genes simultaneously (Blackmore et al., 2012; Lerch et al., 2012; Tang et al., 2009).

In the present study we targeted nine genes for overexpression in CNS neurons singly and in pairwise combinations. In these experiments, the combination of JUN and signal transducer and activator of

Abbreviations: JUN, Jun oncogene; GAP43, growth associated protein 43; ITGA7, integrin alpha 7; PN, postnatal day; SOCS3, suppressor of cytokine signaling 3; KLFs, Krüppel-like transcription factors; PTEN, phosphatase and tensin homologue; DRG, dorsal root ganglion; CGNs, cerebellar granular neurons; TF, transcription factor; Oxr1, oxidase resistance 1; BHLHE40, basic helix-loop-helix family member e40.

* Correspondence to: J. Bixby, University of Miami, 1400 NW 12th Ave, Miami, FL 33136, USA.
** Correspondence to: V.P. Lemmon, The Miami Project to Cure Paralysis, 1095 NW 14th Terrace, Miami, FL 33136, USA. Fax: +1 305 243 3921.
E-mail addresses: jbixby@med.miami.edu (J.L. Bixby), vlemmon@med.miami.edu (V.P. Lemmon).

http://dx.doi.org/10.1016/j.mcn.2014.02.002
1044-7431/

transcription 6 (STAT6) increased total neurite length in disassociated cortical neurons. In organotypic cortical slice cultures, JUN alone promoted growth as well as the JUN/STAT6 combination. JUN is thought to act transcriptionally, as homo- or heterodimers, at AP-1 binding sites (Rauscher et al., 1988). Interestingly, while cortical slices transduced with JUN have similar numbers of surviving neurons and showed increased JUN mRNA and protein, expression of two potential downstream targets (growth associated protein 43 [GAP43] and integrin alpha 7 [ITGA7]) were unchanged and decreased, respectively. Overall, this study demonstrates that JUN can promote axon growth and regeneration in cortical neurons, and suggests that it does so in a way that is mechanistically distinct from what is observed in peripheral axons.

Results

Transcription factor combination overexpression screen in postnatal cortical neurons identifies JUN as potential regulator of CNS neuron axon growth

One way to change the phenotype of a cell is to systematically target individual genes for overexpression. Transcription factors (TFs) are useful targets because they have the potential to mediate widespread changes in gene expression. Our laboratory has used transcription factor overexpression followed by neuronal morphology analysis on both permissive (poly-D-lysine and/or laminin) and inhibitory substrates (chondroitin sulfate proteoglycans, CSPGs) to identify key TFs involved in axon growth (Blackmore et al., 2010, 2012; Buchser et al., 2012; Smith et al., 2011). In the present study we examined eight transcription factors and one small GTPase because when they were individually overexpressed in other assays in our lab they modestly enhanced CNS neuron neurite outgrowth (Table 1 and Supplementary Fig. 1, Blackmore et al., 2010; Smith et al., 2011). We overexpressed two genes simultaneously and could subsequently identify neurons transfected with both genes by exploiting the 2A-peptide labeling strategy (Tang et al., 2009). The coding DNA sequence of the transcription factor was placed upstream of the 2A-mCherry or the 2A-enhanced green fluorescent protein (EGFP) sequence. Appropriate expression of the test proteins and the mCherry or EGFP reporter for each plasmid was verified by transfection into HEK293 cells (examples shown for JUN and STAT6; Fig. 1A,B).

Next we examined the effect of transcription factor overexpression on cortical neuron neurite growth. This experiment was performed in primary postnatal day 3 (PN3) cortical neurons. This age was chosen because primary cultures from adult neurons have low viability and transfection experiments are impractical. In addition these neurons have proven effective in past studies for identifying gene targets involved in axon regeneration (Blackmore et al., 2010; Moore et al., 2009) In each experiment two transcription factor plasmids were electroporated in pairwise combinations, or individual transcription factors were electroporated together with a neutral control cDNA, oxidase resistance 1 (*Oxr1*). This gene has no appreciable effect on neurite outgrowth when overexpressed in cortical neurons (Blackmore et al., 2010). Plasmid ratios were kept at 1:1 yielding co-transfection rates around 80%, as assessed by expression of reporter genes from each plasmid (Fig. 2A, thick arrows). Neurite length measurements were taken from cells expressing both plasmids (e.g., Fig. 2A), and normalized to neurite lengths for neurons expressing two control genes-OXR1 and an enhanced blue fluorescent protein (OXR1-2A-EGFP/mCherry:

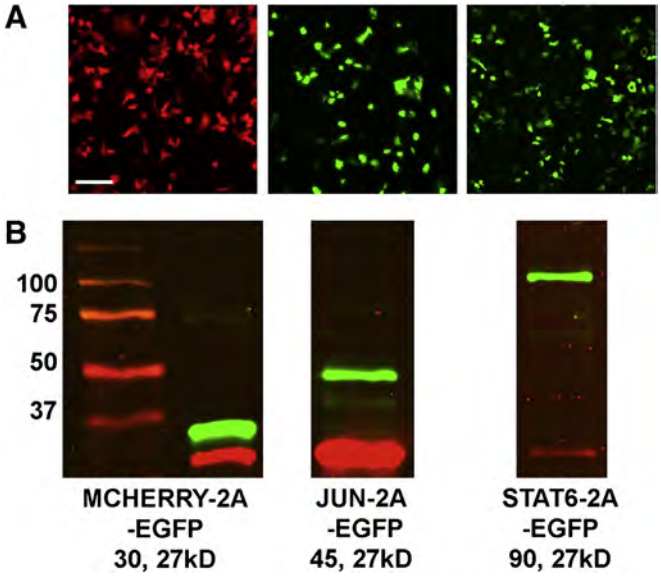

Fig. 1. Transcription factors and a fluorescent reporter are faithfully expressed from 2A-containing plasmids. (A) HEK293 cells were transfected with a single plasmid encoding the transcription factor-2A EGFP or 2A-mCherry. HEK293 cells transfected with mCherry-2A-EGFP, JUN-2A-EGFP or STAT6-2A-EGFP are shown. For mCherry-2A-EGFP, the mCherry channel is shown, for the others, the EGFP channel is shown. Fluorescent reporter expression was verified visually and then protein was harvested for Western blot analysis. Scale bar = 100um. (B) Western blot to verify protein expression. Predicted protein sizes are shifted due to the partial 2A peptide sequence (EGRGSLLTCGDVEENPG) retained on the protein encoded 5′ of the EGFP sequence. The predicted sizes are shown for the first and second proteins respectively. The blots were probed with a polyclonal rabbit-anti-2A antibody which recognizes the partial 2A sequence (Millipore, ABS31) and mouse-anti-EGFP (Clontech, Cat#63238) followed by anti-mouse IR700 (red; LiCOR) and anti-rabbit-IR800 (green; LiCOR).

Table 1
List of genes overexpressed in cortical neurons, their Official Gene Symbol and the neuronal type and substrate where the increase in neurite length was previously observed (Supplemental Fig. 1). Effects were observed in dissociated hippocampal neurons (HPs), cortical neurons (CTs), and cerebellar granular neurons (CGNs) when grown in tissue culture dishes coated with either poly-D-lysine then laminin (LN) or LN and chondroitan sulfate proteoglycans (CSPGs). BHLHE40, JUN and STAT6 increased neurite length in CTs on LN; DCX increased neurite length in CTs on LN; JUN, MYC, and STAT3 increased neurite length in CGNs on LN; BHLHE40 and MYC increased neurite length in HPs on LN; and JUN, MYC, RHEB, STAT3, and STAT6 increased neurite length in HPs grown on CSPGs.

Gene name	Gene symbol	Effect, cell type and substrate
Basic helix-loop-helix family, member e40	*Bhlhe40*	↑ CT on LN; ↑ HP on LN
Doublecortin	*Dcx*	↑ CT on LN
Iroquois Related Homeobox 3	*Irx3*	Not tested
Jun Oncogene	*Jun*	↑ HP neurons on CSPGs; ↑ CT on LN; ↑ HP on LN
Krüppel-like Factor 6	*Klf6*	↑ CT on LN
Krüppel-like Factor 7	*Klf7*	↑ CT neurons, LN
Myelocytomatosis Oncogene	*Myc*	↑ HP neurons, CSPGs; ↑ CGNs on LN
Oxidation Resistance 1	*Oxr1*	No effect over numerous experiments
Ras Homolog Enriched in Brain	*Rheb*	↑ HP neurons, CSPGs
Signal Transducer and Activator of Transcription 3	*Stat3*	↑ CGNs on LN
Signal Transducer and Activator of Transcription 6	*Stat6*	↑ HP neurons on CSPGs; ↑ CT on LN
SMAD Family Member 1	*Smad1*	Not tested

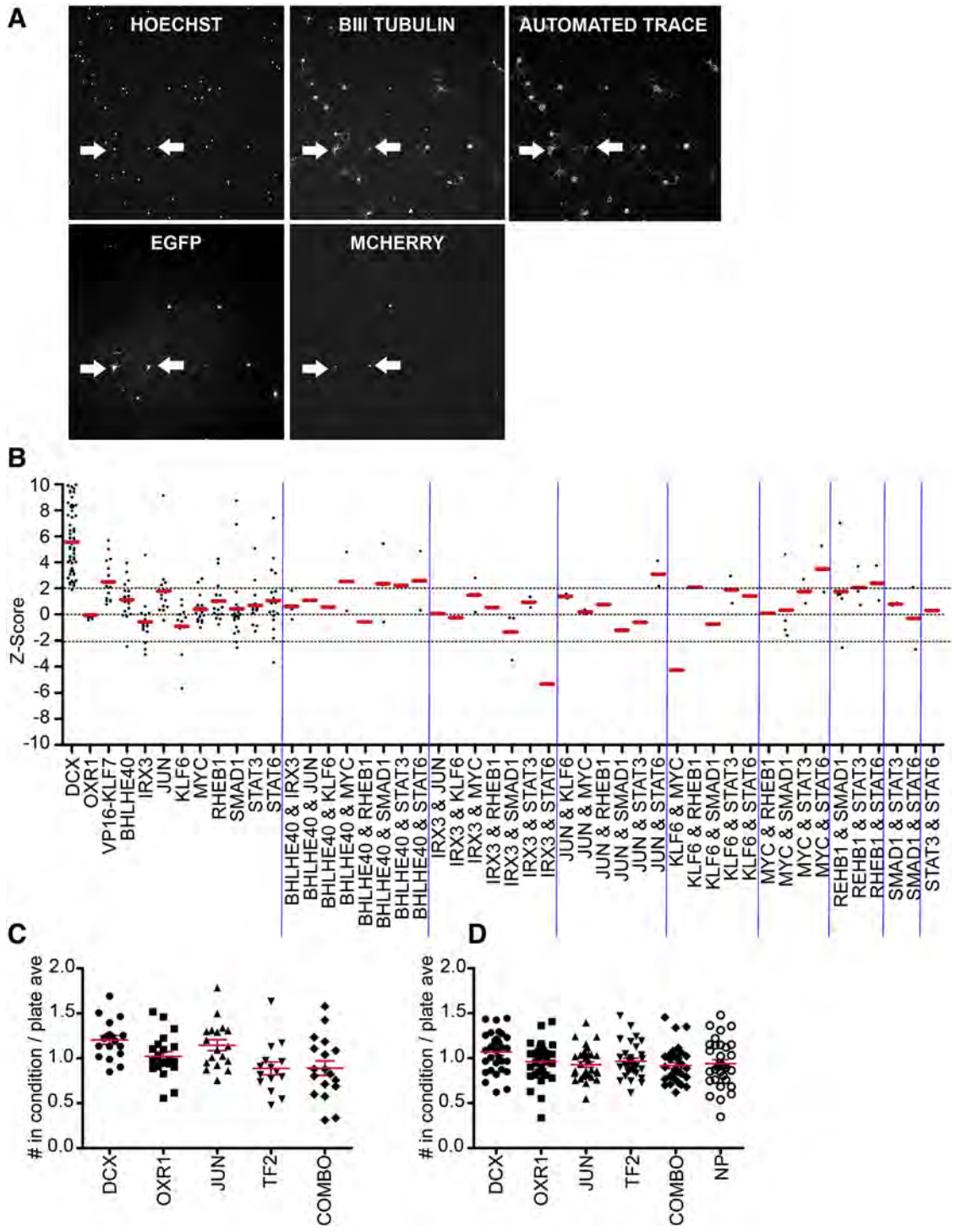

Fig. 2. The JUN/STAT6 transcription factor combination increases neurite length in primary cortical neurons. (A) Representative images of early PN3 cortical neurons after transfection, immunostaining, and image acquisition and analysis on a Cellomics ArrayScanVTI (nuclear stain: Hoechst; neuronal processes: βIII-tubulin, DCX-2A-EGFP transfection: EGFP; OXR1-2A-mCherry transfection, mCherry). Thick arrows show examples of neurons positive for both EGFP and mCherry. (B) DCX and VP16-KLF7 consistently increased neurite length after transfection. OXR1 has no effect on neurite length. The average Z-Score (Ave Total Neurite length TF Combo — Ave Total Neurite length OXR1/EBFP)/OXR1/EBFP Stdev) for each transcription factor or transcription factor combination is shown with a red dash. Individual experimental results are shown as black dots. Dashed black line indicates Z-Scores of +/−2.0. (C) The number of transfected cells surviving after JUN transfection is not different than other plasmid combinations (labeled as COMBO) or controls (DCX and OXR1). One-Way ANOVA, with Bonferroni's Multiple Comparison Test, *P < 0.01 for DCX and COMBO, **P < 0.001 for DCX and TF2. (D) The number of neurons surviving per well for each condition is not different. Red bars reflect mean +/− s.e.m. TF2 — transcription factor 2; NP — no plasmid.

EBFP-2A-EGFP/mCherry). The cytoskeletal binding protein Doublecortin (DCX) and a transcriptionally active Krüppel-like factor 7 (VP16-KLF7; Blackmore et al., 2010, 2012) were included as positive controls because they reliably increase total neurite length (Fig. 2B). The majority of transcription factors did not actively repress neurite outgrowth. This result is expected since these transcription factors were chosen for combinatorial overexpression because of their ability to promote neurite growth in previous experiments (Supplemental Fig. 1, Table 1). For example, the basic helix-loop-helix family member e40 (BHLHE40) increased neurite growth in both dissociated cortical neurons and in hippocampal

neurons growing on inhibitory CSPGs (Supplemental Fig. 1). However, combinations including BHLHE40 were inconsistent in their ability to promote neurite growth. The only TF pair that increased neurite growth in several experiments was JUN/STAT6 (Z-Score Ave = 3.11, Fig. 2B). Neurons transfected with either JUN or STAT6 showed variable neurite lengths. However, of the transcription factors expressed alone, JUN gave the highest mean Z-Score (Z = 1.78, Fig. 2B), while STAT6 alone had no consistent effect. To determine if JUN altered neuronal survival we examined the number of transfected neurons and the total number of neurons in each well. If JUN promoted survival, the numbers of neurons after transfection (Fig. 2C) and the total number of neurons surviving in JUN transfected wells should be greater than in controls (Fig. 2D), but this was not the case. Taken together these experiments show that JUN has a variable, but generally positive impact on neurite length, does not affect neuronal survival after transfection, and when co-expressed with STAT6 can increase total neurite length in primary cortical neurons.

After viral transduction Jun transcript and protein are overexpressed in ex vivo cortical slice cultures

The previous observation, along with the fact that JUN has been implicated in peripheral nerve regeneration, led us to further test JUN's role in CNS axon growth, using an organotypic cortical slice model (Al-Ali et al., 2013; Blackmore et al., 2012). In this model PN5 cortical slices are "matured" for 1 week in vitro, after which they are injured by transection, and transected halves are allowed to fuse (Fig. 3A and Experimental Methods). Since we hypothesized that JUN overexpression would promote axon growth, we first assessed endogenous JUN expression during the 15 days in culture, corresponding to the time course of the experiment. JUN transcript levels did not significantly change during this time, either before or after the injury (Fig. 3B). We also examined the expression of two potential transcriptional targets: GAP43, whose expression is highly correlated with axon regeneration (Campbell et al., 1991; Schaden et al., 1994; Weber and Skene, 1998); and ITGA7, another potential downstream transcriptional effector of JUN (Raivich et al., 2004) that has been implicated in axon regeneration (Ekstrom et al., 2003; Raivich et al., 2004; Tan et al., 2011). GAP43 expression significantly and substantially decreased in cortical slices maintained for 8 and 15 days. Cortical slice injury did not further alter GAP43 transcript level (Fig. 3C). While ITGA7 expression was slightly more variable, it did not significantly change over the course of the experiment (One-way ANOVA, p = 0.344; Fig. 3D).

Next, we established that viral JUN transduction would indeed increase JUN expression in cortical slices. We made AAV8 virus with the JUN-2A-mCherry plasmid, the same JUN plasmid used in the previous experiments. JUN immunoreactivity was undetectable in naive cortical slices, in injured cortical slices, and in cortical slices transduced with pAAV8-VP16-KLF7, but was readily observed in neurons after JUN transduction (Fig. 4A,B). In accordance with this observation, JUN mRNA levels were nearly 50-fold higher in slices transduced with the JUN viral particles (Fig. 4C).

Jun promotes CNS neuron axon growth in cortical slice cultures

The same cortical slice model was used to examine the effect of JUN overexpression on CNS axon growth. Cortical slices were virally transduced to overexpress each plasmid, then cut in half to axotomize the axons at the corpus collosum and each slice half was paired with a naive, unlabeled cortical slice half, after which the number of axons growing into the unlabeled side was quantified (Fig. 5A and as in Blackmore et al., 2012). After JUN transduction, the number of axons growing into the unlabeled cortical half was increased more than 3-fold (Fig. 5B,C). VP16-KLF7 also significantly increased the number of growing axons, supporting the in vitro data and previous observations (Blackmore et al., 2012). As anticipated, OXR1 produced no increase in the number of axons growing into the unlabeled side (Fig. 5B,C). Importantly, the number of GFP+ neurons detected in each slice was not different in the various conditions (Fig. 4D,E), consistent with our observations that the number of transfected neurons and surviving neurons per well was not altered by JUN transfection in dissociated neurons (Fig. 2C,D). To examine whether increased axon growth was due to JUN transcriptional activity and not just increased transcriptional activity from any transcription factor we generated virus from the IRX3- and SMAD1-2A-mCherry plasmids. The number of axons growing in organotypic cortical slice cultures after IRX3 transduction was slightly, but not significantly reduced (Fig. 5B), which mirrors the observation in dissociated cortical neurons (Fig. 2B, Z-score mean = −0.73). SMAD1 had no appreciable effect on neurite growth in dissociated cortical neurons and indeed, cortical neurons transduced with SMAD1 grew similar numbers of axons as OXR1 and EBFP controls (Fig. 5B,C).

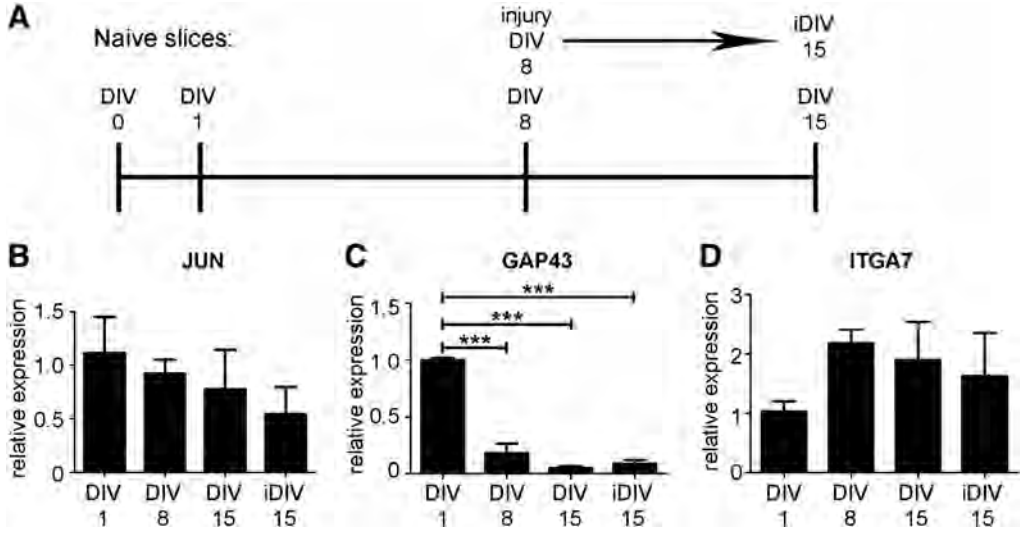

Fig. 3. JUN and ITGA7 mRNA expression do not change in uninjured or injured cortical slice cultures while GAP43 mRNA decreases by 8 days (A) Experimental timeline. Cortical slices were isolated from PN5 pups (DIV0) and cultured before RNA collection. RNA was isolated at 1, 8, and 15 days in vitro (DIV) for gene expression analysis. A set of cortical slices were cut in half at DIV8 before RNA harvest at DIV15 (iDIV15) to examine the effect of injury on gene expression. (B) qRT-PCR analysis for (B) JUN, (C) GAP43, and (D) ITGA7. ***P < 0.0001, One-way ANOVA followed by Dunnett's Multiple Comparison Test. N = 3 slices.

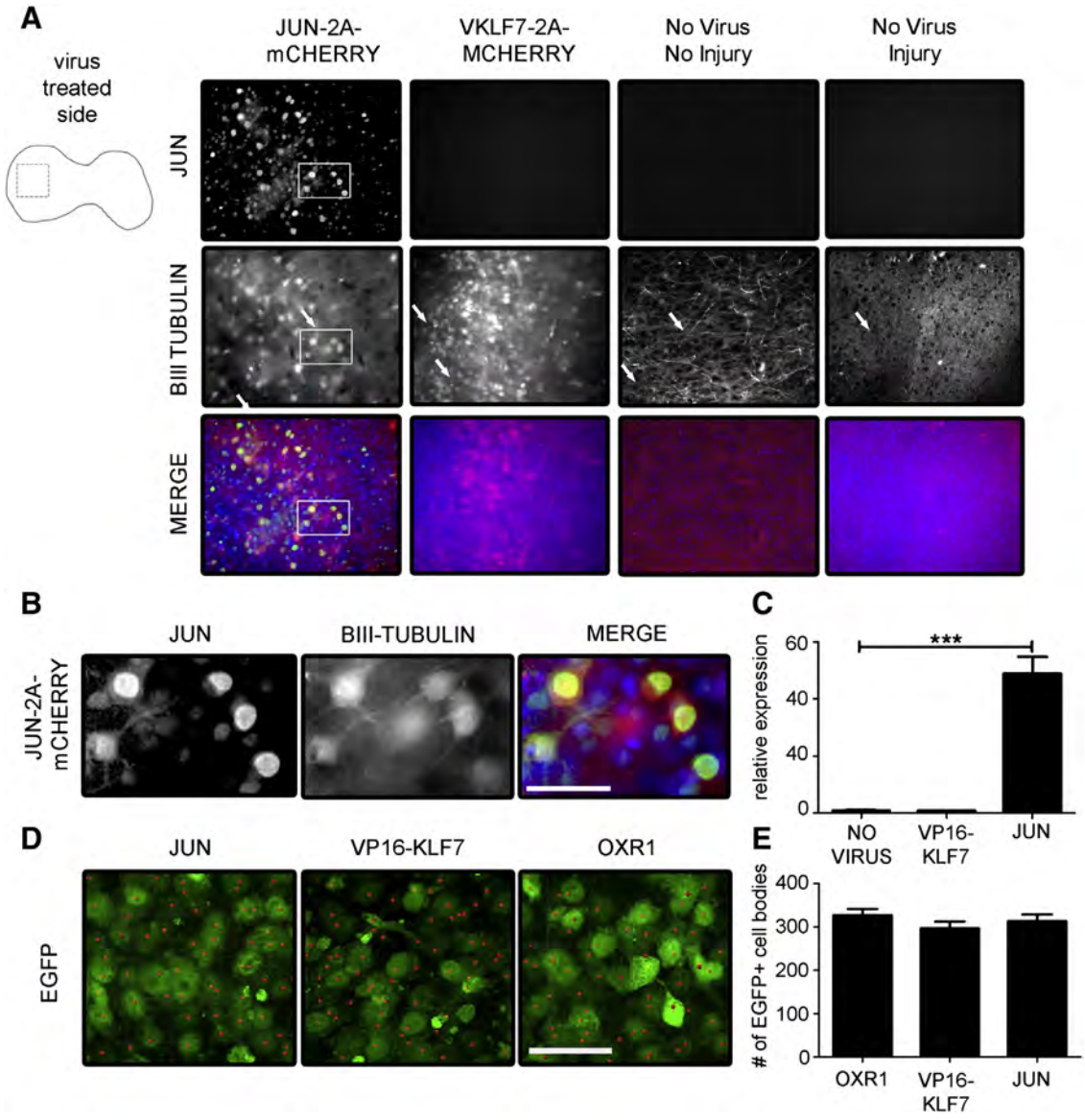

Fig. 4. JUN is overexpressed in cortical neurons after viral transduction with pAAV8-JUN-2A-mCherry. (A) Schematic showing ROI for images taken in the cortical slices (dashed box). A mouse monoclonal antibody to JUN protein labels cortical neurons in slices that were treated with pAAV8-JUN-2A-mCherry viral particles that preferentially target cortical neurons (Blackmore et al., 2012). Neuronal specific βIII-Tubulin labels neuronal process (arrows). Exposure times were kept constant between conditions. Scale bar = 20um (B) Higher magnification images of ROIs from boxes in (A) Scale bar = 10um. Cortical slices were immunostained for JUN, βIII-Tubulin and DAPI (shown only in MERGE). (C) JUN transcript expression was significantly increased in cortical slices after JUN viral transduction. ***P < 0.0005, One-way ANOVA followed by Dunnett's Multiple Comparison Test. N = 3 slices. (D) Three-dimensional confocal stack of OXR1, VP16-KLF7, and JUN transduced slices. Red dots show neurons identified and counted by the Imaris software. Scale bar = 40um. (E) EGFP+ cell number is similar in cortical slices transduced with OXR1, VP16-KLF7, or JUN. N = 3 experiments; 6 slices per viral treatment.

In an effort to understand how JUN overexpression may be affecting downstream gene expression to promote axon growth we examined mRNA expression for GAP43 and ITGA7. Interestingly, GAP43 expression was unchanged while ITGA7 expression was decreased after either VP16-KLF7 or JUN transduction (Fig. 5D,E). This indicates that JUN overexpression in CNS neurons increases axon growth but is not associated with increases in GAP43 or ITGA7 mRNA expression.

Discussion

Despite years of work examining JUN's relationship with axon growth and regeneration, gain of function studies directly testing a role for JUN in this process are surprisingly lacking. Here we discover a role for JUN in promoting cortical neuron neurite growth when overexpressed. JUN slightly increased neurite growth in dissociated cortical neurons. To test JUN's ability to promote axon growth in a more in vivo-like environment, we examined the effect of JUN overexpression on the growth of axons in an organotypic cortical slice injury model. In this model the effect of JUN was more striking, increasing growth to a greater extent than the positive control, a transcriptionally active form of KLF7 that has been shown to promote regeneration in vivo (Blackmore et al., 2012). Interestingly, expression of JUN targets implicated in axon growth, GAP43 and ITGA7 (Raivich et al., 2004; Weber and Skene, 1998), did not increase when JUN was overexpressed. Overall these findings indicate that JUN can drive axonal growth in CNS neurons and suggests that the mechanisms through which JUN is acting are not identical to those seen previously in peripheral axons (Raivich et al., 2004; Schreyer and Skene, 1991).

We focused our analysis on JUN alone because expression of STAT6 did not affect neurite growth in dissociated cortical neurons,

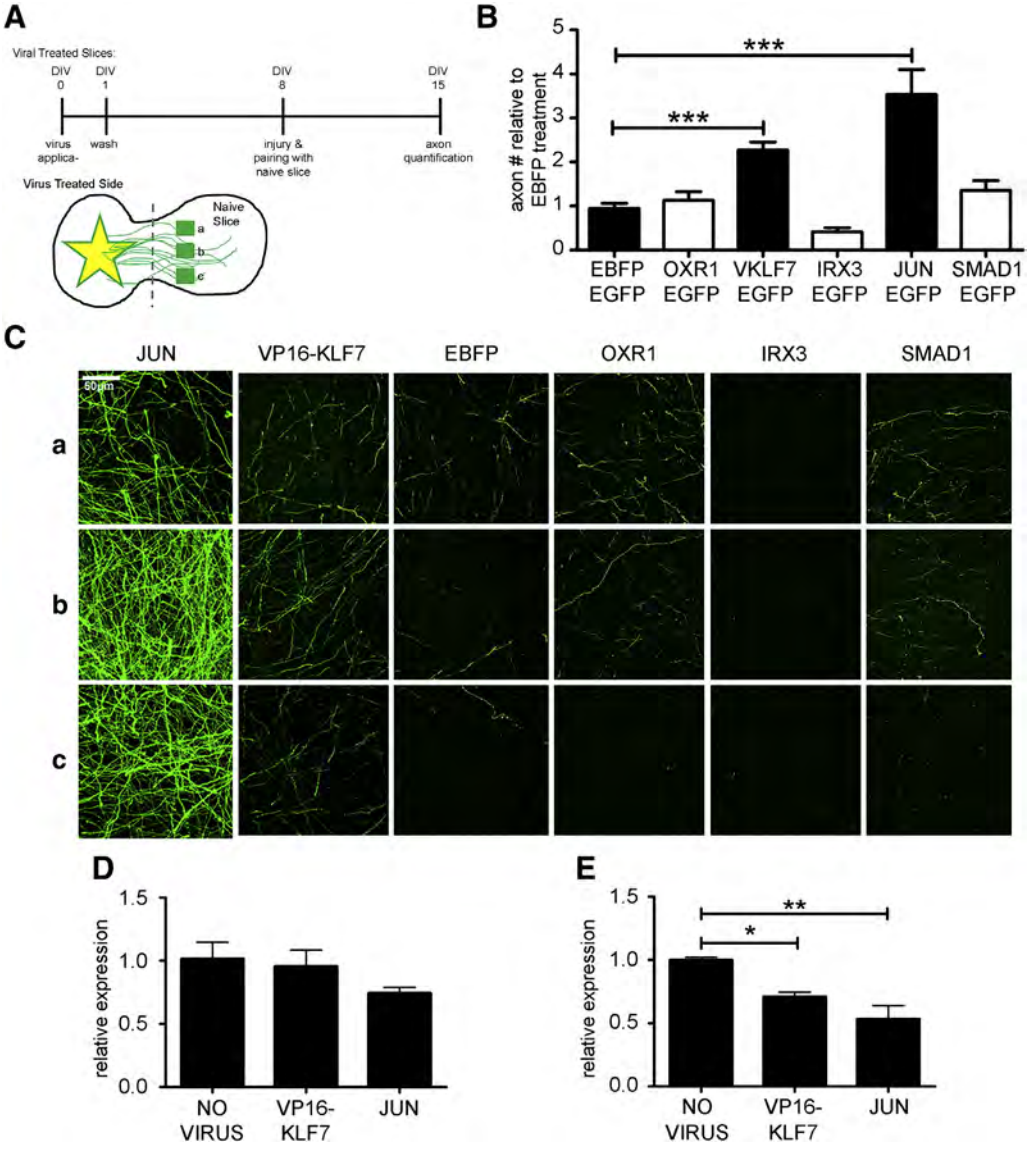

Fig. 5. Overexpression of JUN in injured cortical slices increases axon growth into an adjoining cortical slice. (A) Timeline of viral treatment and injury, and a schematic showing ROIs for quantification of axon number. (B) Quantification of the number of axons normalized to the number observed in slices treated with enhanced blue fluorescent protein (EBFP) and EGFP. N = 32 slices for EBFP, VP16-KLF7 (VKLF7); N = 20 for JUN; and N = 12 for OXR1, IRX3, and SMAD1. (C) Confocal z-stack images of EGFP labeled axons crossing into regions (a), (b), and (c) in the untransduced naive slice. Viral particle treatment combinations are labeled. (D) GAP43 transcript mRNA level does not change. (E) ITGA7 transcript is reduced after VP16-KLF7 or JUN treatment. *P < 0.05, **P < 0.005, ***P < 0.0005, One-way ANOVA followed by Dunnett's Multiple Comparison Test. N = 3 slices.

nor did it significantly increase axon growth in the cortical slice model (axon # relative to EBFP treatment = 2.05 ± 0.32 sem; N = 20; Supplemental Fig. 3). In addition, the effect on axon growth after combinatorial transduction of JUN and STAT6 was comparable to JUN treatment alone (axon # relative to EBFP treatment: 3.58 ± 0.48 vs. 3.52 ± 0.57; N = 20, ***P < 0.0005; Supplemental Fig. 3). Interestingly, in JUN/STAT6 transduced cortical slices JUN mRNA levels were significantly increased above those detected with JUN treatment alone (Supplemental Fig. 2). This suggests that STAT6 either stabilizes or promotes JUN mRNA expression. In contrast, while STAT6 mRNA levels were increased 10,000-fold after STAT6 transduction, they did not further increase when JUN and STAT6 were combined (Supplemental Fig. 2).

JUN expression increases after either CNS or PNS neuronal injury, contributing to the idea that JUN is involved in axon regeneration. For example, after sciatic nerve crush, there is a sustained increase in both JUN mRNA and protein (Jenkins and Hunt, 1991). In addition, JUN expression increases only when the peripheral, but not the central branch, of a sensory neuron is lesioned, associating JUN with axon regeneration (Broude et al., 1997). This idea is supported by the observation that JUN is expressed in retinal ganglion cells growing into peripheral nerve graphs and is upregulated again when they are re-axotomized months later (Robinson, 1994, 1995; Schaden et al., 1994). Indeed, several groups knocked out JUN in populations of neurons that normally regenerate, and found that JUN was necessary for facial motor neuron axonal regeneration, target reinnervation and functional recovery (Raivich et al., 2004; Ruff et al., 2012). More recently, it was demonstrated that Schwann cell JUN function is critical for successful peripheral nerve regeneration (Arthur-Farraj et al., 2012; Fontana et al., 2012).

While these studies examine JUN's expression and loss of function in populations of cells that are normally regenerating no one has previously tested the effect of JUN gain of function on axonal regeneration. Testing gain of function is challenging because it can be difficult to demonstrate that the protein is expressed and activated. We clearly show that both JUN mRNA and protein are increased after viral

transduction. In cortical slices JUN protein detection is most recognizable in cells that appear to be neuronal (Fig. 4B). While we have found that AAV8 preferentially labels cortical neurons (Blackmore et al., 2012), an observation that is consistent with previous reports on AAV8 tropism (Howard et al., 2008; Taymans et al., 2007), we cannot rule out the possibility that JUN expression in glia cells (e.g. in virally transduced astrocytes or oligodendrocytes) contributes to the increased axonal growth we observed. It was recently demonstrated that JUN expression in Schwann cells mediates peripheral and motor neuron regeneration (Arthur-Farraj et al., 2012; Fontana et al., 2012). However, this seems unlikely given the neuronal morphology of cells expressing JUN, and the expression in transduced cells of BIII tubulin (Fig. 4B). To rule out the possibility that the increased axon regeneration reflected an increase in neuronal survival in JUN-treated cortical slices, we examined the number of GFP + neurons after viral transduction (Fig. 4D,E). We found no differences in neuronal number between slices transduced to express JUN and those transduced with other TFs, suggesting that JUN overexpression did not promote increased survival.

In cortical slices GAP43 mRNA levels decrease substantially after 1 week in culture, consistent with previous observations documenting a developmental decline in GAP43 expression (Karimi-Abdolrezaee and Schreyer, 2002; Karimi-Abdolrezaee et al., 2002). In regenerating retinal ganglion cells, increases in JUN expression are coincident with increases in GAP43 expression (Schaden et al., 1994) and we find predicted JUN/AP1 transcription factor binding sites (TFBSs) in the GAP43 promoter (see Experimental Methods), consistent with a previous study (Weber and Skene, 1998). Thus we were surprised that JUN expression and increased cortical axon growth were not correlated with increases in expression of GAP43. We also examined expression of ITGA7, another transcript whose upregulation is associated with increases in JUN expression (Ekstrom et al., 2003), and which is a potential JUN transcription target (Raivich et al., 2004); and we found multiple predicted AP1 transcription factor binding sites in the ITGA7 promoter (see Experimental Methods). Interestingly, we found that ITGA7 expression decreased with JUN overexpression, suggesting that JUN may be actually repressing ITGA7's expression. This observation is in contrast to observations in peripheral neurons (Raivich et al., 2004), suggesting that JUN mediated CNS axon growth is either driven by different transcriptional targets in the CNS, that forcing JUN overexpression alters how JUN hetero- and homodimers effect downstream gene expression, or that JUN is mediating its effects on CNS axon growth independently of transcription. Overall this study demonstrates that JUN gain of function in CNS neurons can result in increased axon growth, and appears to do so without the increases in GAP43 and ITGA7 expression observed in other regenerating neuronal populations.

Experimental methods

All animal work was performed according to the AVMA guidelines and University of Miami IACUC approved protocols.

Table 2
Equal numbers of viral genomes were applied to each cortical slice (3.0E +13 genomes/μL/side of the cortex).

AAV8 particles
ANTI-LUC-2A-EGFP
EBFP-2A-MCHERRY
IRX3-2A-MCHERRY
JUN-2A-MCHERRY
OXR1-2A-MCHERRY
SMAD1-2A-MCHERRY
VP16-KLF7-2A-MCHERRY

Cortical neuron transfection

Postnatal day 3 (PN3) rat pups were euthanized, cortices were removed and primary cortical neurons were isolated and transfected as previously described (Blackmore et al., 2010). Briefly, a square wave pulse (350 V, 350 μs; Harvard Apparatus/BTX #45-0450) was applied to 50,000 cortical neurons resuspended in intraneuronal buffer (135 mM KCl, 0.2 mM CaCl2, 2 mM MgCl2, 10 mM HEPES, 5 mM EGTA, pH7.3) containing a total of 6 μg of plasmid DNA (3 μg of each plasmid) for each condition. Cells were transferred to 24-well tissue culture plates (10,000cells/well) coated with 1 mg/mL poly-D-lysine (Invitrogen) with Neurobasal media (Lonza) supplemented with neural cell survival factor 1 (NSF-1, Lonza) and grown for 72 h, then fixed and immunostained with a neuronal specific mouse monoclonal beta-III tubulin antibody (1:500; produced in house) and AlexaFluor647 secondary (1:1000; Invitrogen). Images were captured on a Cellomics ArrayScanVTI automated microscope and neuronal morphology was assessed with the Neuronal Profiling Algorithm (ThermoFisher). Total neurite length (TNL) was automatically captured for each transfected neuron. For each experimental condition a minimum of 100 cells was analyzed and the average TNL was calculated (TNL_{mean}) for each transfection condition. Neurite lengths were compared as Z-Scores ($Z = x - u / \sigma$; $x = TNL_{TF\ Combo}$; $u = TNL_{Control}$; $\sigma =$ standard deviation of $TNL_{Control}$). We considered increases in neurite growth statistically significant if they were more than 2 standard deviations (2 Z-Scores) above the mean of the control (Oxidase resistance 1/enhanced blue fluorescent protein).

Cortical slice culture axon and GFP + cell counts

Between six and eight 350 μm coronal cortical slices were made from each brain of PN5 Sprague Dawley rat pups using a tissue chopper (Blackmore et al., 2012). Cortical slices were then further dissected so that only the cortex and corpus callosum remained. The sections were carefully placed in Millicell culture inserts inside 35 mm Petri dishes with culture media made from Basal Medium, Eagles (Gibco), Hanks Balanced Salt Solution, and horse serum (Gibco), and NeuroCult™ SM1 Neuronal Supplement (Stemcell Technologies), L-glutamine (Invitrogen), D-glucose and pen/strep (Invitrogen). One microliter of viral particles (3.0E + 13 viral genomes; Table 2) was applied to each side of the cortex 2–3 h after plating. After 24 h the slices were washed to remove residual viral particles and maintained for an additional week. Cortices transduced with viral particles were cut in half and paired with untransduced cortical tissue slices so that the two pieces were in physical contact, and were cultured for another week. Cortical slices were fixed with 4% paraformaldehyde in phosphate buffered saline, pH 7.4 and mounted onto glass slides with coverslips. For axon counts: three regions of interest (ROI; 210 μm^2) each 1 mm from the border between the 2 halves of the slice were imaged on a confocal microscope (60×) through all Z-planes. The combined number of processes crossing a vertical and a horizontal line through the center of each ROI was quantified (Fig. 5A). This number was normalized to the number counted in control EBFP transduced slices processed in the same experimental batch. For GFP + neuron counts: three areas 1 mm and three areas 2 mm away from border between the 2 halves of the slice were imaged on a confocal microscope (60× objective) through all Z-planes (Z-plane thickness = 1.2 um). The GFP + cells were counted using Imaris ×64, version 7.6.5 (BITPLANE Scientific Software). The "spots" function was used to recognize the GFP + cells using a spot diameter of at least 4.14 μm. All the images were corrected for double counted cells or counted artifacts by manual inspection.

Quantitative reverse transcriptase polymerase chain reaction (qRT-PCR)

Cortical slices were obtained and treated as above. RNA was extracted after tissue homogenization using Trizol Reagent (Invitrogen). CDNA was made from 500 ng of RNA using the Advantage RT for PCR Kit (Clontech).

Primers were designed to span introns and a no-RT control was run for every primer set to check for DNA contamination. Primer efficiencies were determined using a standard curve method and the delta delta Ct method was used for determine fold change. The following primers (5′ → 3') were used: JUN: GAGTCTCAGGAGCGGATCAA, TGAGTTGGCA CCCACTGTTA; GAP43: GGCTCTGCTACTACCGATGC, GACGGCGAGTTATC AGTGGT; ITGA7: CTCTTTGCTTGTCCCCTGAG, GCAGAACCCAAATTGTTC GT. STAT6: ATGCCAAAGCCACTATCCTG, ATCAAACCACTGCCAAAAGG.

Transcription factor binding site prediction

The GAP43 and ITGA7 promoter (−1000 bp/+300 bp from the transcription start site) DNA sequences were retrieved from the UCSC Genome Browser (http://genome.ucsc.edu/) and input into JASPAR (Bryne et al., 2008), which predicts transcription factor binding site matrices (TFBSs). JASPAR predicts four AP1 (Fos/Jun/ATF) TFBSs in the mouse GAP43 promoter, five in the rat GAP43 promoter, five in the mouse ITGA7 promoter and six in the rat ITGA7 promoter.

Western blot

HEK293 cells were transfected with Lipofectamine Reagent (Invitrogen) according to the manufacturer's recommendation. Cells were lysed in boiling SDS sample buffer and samples were electrophoresed on 10% SDS-polyacrylamide gels at 100 V until the dye front reached the bottom of the gel. Transfers were performed overnight in 2.2 M bicarbonate buffer at 20 V. Immunoblotting was performed with appropriate primary and secondary antibodies (primary antibodies: rabbit polyclonal to 2A, 1:5000 (Millipore #09-085); mouse monoclonal to GFP, 1:2000 (Clontech #63238); secondary antibodies: anti-mouse/-rabbit-IR700 or -IR800, 1:5000; (Li-COR # 926–32210, #926-32211, #926-68071, and #926-68072)). Blots were scanned on an Odyssey Imaging system and band intensities were analyzed using Odyssey system software (Li-COR).

Jun immunohistochemistry

Cortical slices were treated and fixed as described above. Slices were processed with mouse monoclonal antibody to JUN (BD Biosciences #610362) and rabbit polyclonal antibody to βIII-tubulin (Sigma #T2200) after antigen retrieval with 10 mM sodium citrate, pH9.0 at 80 °C for 30 min. Secondary antibodies were goat-anti mouse Alexa Fluor 488 and goat-anti rabbit Alexa Fluor 546 (Life Technologies #A-21049 and #A-21085). Nuclei were visualized with DAPI.

Supplementary data to this article can be found online at http://dx.doi.org/10.1016/j.mcn.2014.02.002.

Acknowledgements

We thank Edna Gamliel for technical assistance. This work was supported by the National Institutes of Health grants HD057521 (to V.P.L), and NS059866 (to J.L.B.), DOD grant W81XWH-05-1-0061 (to V.P.L. and J.L.B.), the Buoniconti Fund and the Walter G. Ross Distinguished Chair in Developmental Neuroscience (to V.P.L).

References

Al-Ali, H., Schürer, S.C., Lemmon, V.P., Bixby, J.L., 2013. Chemical interrogation of the neuronal kinome using a primary cell-based screening assay. ACS Chem. Biol. 8 (5), 1027–1036.

Arthur-Farraj, P.J., Latouche, M., Wilton, D.K., Quintes, S., Chabrol, E., Banerjee, A., Woodhoo, A., Jenkins, B., Rahman, M., Turmaine, M., Wicher, G.K., Mitter, R., Greensmith, L., Behrens, A., Raivich, G., Mirsky, R., Jessen, K.R., 2012. c-Jun reprograms Schwann cells of injured nerves to generate a repair cell essential for regeneration. Neuron 75, 633–647.

Bareyre, F.M., Garzorz, N., Lang, C., Misgeld, T., Buning, H., Kerschensteiner, M., 2011. In vivo imaging reveals a phase-specific role of STAT3 during central and peripheral nervous system axon regeneration. Proc. Natl. Acad. Sci. U. S. A. 108, 6282–6287.

Blackmore, M., Letourneau, P.C., 2006. Changes within maturing neurons limit axonal regeneration in the developing spinal cord. J. Neurobiol. 66, 348–360.

Blackmore, M.G., Moore, D.L., Smith, R.P., Goldberg, J.L., Bixby, J.L., Lemmon, V.P., 2010. High content screening of cortical neurons identifies novel regulators of axon growth. Mol. Cell. Neurosci. 44, 43–54.

Blackmore, M.G., Wang, Z., Lerch, J.K., Motti, D., Zhang, Y.P., Shields, C.B., Lee, J.K., Goldberg, J.L., Lemmon, V.P., Bixby, J.L., 2012. Kruppel-like Factor 7 engineered for transcriptional activation promotes axon regeneration in the adult corticospinal tract. Proc. Natl. Acad. Sci. U. S. A. 109, 7517–7522.

Broude, E., McAtee, M., Kelley, M.S., Bregman, B.S., 1997. c-Jun expression in adult rat dorsal root ganglion neurons: differential response after central or peripheral axotomy. Exp. Neurol. 148, 367–377.

Bryne, J.C., Valen, E., Tang, M.H., Marstrand, T., Winther, O., da Piedade, I., Krogh, A., Lenhard, B., Sandelin, A., 2008. JASPAR, the open access database of transcription factor-binding profiles: new content and tools in the 2008 update. Nucleic Acids Res. 36, D102–D106.

Buchser, W.J., Smith, R.P., Pardinas, J.R., Haddox, C.L., Hutson, T., Moon, L., Hoffman, S.R., Bixby, J.L., Lemmon, V.P., 2012. Peripheral nervous system genes expressed in central neurons induce growth on inhibitory substrates. PLoS One 7, e38101.

Campbell, G., Anderson, P.N., Turmaine, M., Lieberman, A.R., 1991. GAP-43 in the axons of mammalian CNS neurons regenerating into peripheral nerve grafts. Exp. Brain Res. 87, 67–74.

Chen, D.F., Jhaveri, S., Schneider, G.E., 1995. Intrinsic changes in developing retinal neurons result in regenerative failure of their axons. Proc. Natl. Acad. Sci. U. S. A. 92, 7287–7291.

Davies, S.J., Goucher, D.R., Doller, C., Silver, J., 1999. Robust regeneration of adult sensory axons in degenerating white matter of the adult rat spinal cord. J. Neurosci. 19, 5810–5822.

Ekstrom, P.A., Mayer, U., Panjwani, A., Pountney, D., Pizzey, J., Tonge, D.A., 2003. Involvement of alpha7beta1 integrin in the conditioning-lesion effect on sensory axon regeneration. Mol. Cell. Neurosci. 22, 383–395.

Fontana, X., Hristova, M., Da Costa, C., Patodia, S., Thei, L., Makwana, M., Spencer-Dene, B., Latouche, M., Mirsky, R., Jessen, K.R., Klein, R., Raivich, G., Behrens, A., 2012. c-Jun in Schwann cells promotes axonal regeneration and motoneuron survival *via* paracrine signaling. J. Cell Biol. 198, 127–141.

Goldberg, J.L., Klassen, M.P., Hua, Y., Barres, B.A., 2002. Amacrine-signaled loss of intrinsic axon growth ability by retinal ganglion cells. Science 296, 1860–1864.

GrandPre, T., Nakamura, F., Vartanian, T., Strittmatter, S.M., 2000. Identification of the Nogo inhibitor of axon regeneration as a Reticulon protein. Nature 403, 439–444.

Horn, K.P., Busch, S.A., Hawthorne, A.L., van Rooijen, N., Silver, J., 2008. Another barrier to regeneration in the CNS: activated macrophages induce extensive retraction of dystrophic axons through direct physical interactions. J. Neurosci. 28, 9330–9341.

Howard, D.B., Powers, K., Wang, Y., Harvey, B.K., 2008. Tropism and toxicity of adeno-associated viral vector serotypes 1, 2, 5, 6, 7, 8, and 9 in rat neurons and glia *in vitro*. Virology 372, 24–34.

Jenkins, R., Hunt, S.P., 1991. Long-term increase in the levels of c-jun mRNA and jun protein-like immunoreactivity in motor and sensory neurons following axon damage. Neurosci. Lett. 129, 107–110.

Karimi-Abdolrezaee, S., Schreyer, D.J., 2002. Retrograde repression of growth-associated protein-43 mRNA expression in rat cortical neurons. J. Neurosci. 22, 1816–1822.

Karimi-Abdolrezaee, S., Verge, V.M., Schreyer, D.J., 2002. Developmental down-regulation of GAP-43 expression and timing of target contact in rat corticospinal neurons. Exp. Neurol. 176, 390–401.

Kigerl, K.A., Gensel, J.C., Ankeny, D.P., Alexander, J.K., Donnelly, D.J., Popovich, P.G., 2009. Identification of two distinct macrophage subsets with divergent effects causing either neurotoxicity or regeneration in the injured mouse spinal cord. J. Neurosci. 29, 13435–13444.

Lee, J.K., Geoffroy, C.G., Chan, A.F., Tolentino, K.E., Crawford, M.J., Leal, M.A., Kang, B., Zheng, B., 2010. Assessing spinal axon regeneration and sprouting in Nogo-, MAG-, and OMgp-deficient mice. Neuron 66, 663–670.

Lerch, J.K., Kuo, F., Motti, D., Morris, R., Bixby, J.L., Lemmon, V.P., 2012. Isoform diversity and regulation in peripheral and central neurons revealed through RNA-Seq. PLoS One 7, e30417.

Liu, K., Lu, Y., Lee, J.K., Samara, R., Willenberg, R., Sears-Kraxberger, I., Tedeschi, A., Park, K.K., Jin, D., Cai, B., Xu, B., Connolly, L., Steward, O., Zheng, B., He, Z., 2010. PTEN deletion enhances the regenerative ability of adult corticospinal neurons. Nat. Neurosci. 13, 1075–1081.

Moore, D.L., Blackmore, M.G., Hu, Y., Kaestner, K.H., Bixby, J.L., Lemmon, V.P., Goldberg, J.L., 2009. KLF family members regulate intrinsic axon regeneration ability. Science 326, 298–301.

Park, K.K., Liu, K., Hu, Y., Smith, P.D., Wang, C., Cai, B., Xu, B., Connolly, L., Kramvis, I., Sahin, M., He, Z., 2008. Promoting axon regeneration in the adult CNS by modulation of the PTEN/mTOR pathway. Science 322, 963–966.

Raivich, G., Bohatschek, M., Da Costa, C., Iwata, O., Galiano, M., Hristova, M., Nateri, A.S., Makwana, M., Riera-Sans, L., Wolfer, D.P., Lipp, H.P., Aguzzi, A., Wagner, E.F., Behrens, A., 2004. The AP-1 transcription factor c-Jun is required for efficient axonal regeneration. Neuron 43, 57–67.

Rauscher III, F.J., Voulalas, P.J., Franza Jr., B.R., Curran, T., 1988. Fos and Jun bind cooperatively to the AP-1 site: reconstitution *in vitro*. Genes Dev. 2, 1687–1699.

Robinson, G.A., 1994. Immediate early gene expression in axotomized and regenerating retinal ganglion cells of the adult rat. Brain Res. Mol. Brain Res. 24, 43–54.

Robinson, G.A., 1995. Axotomy-induced regulation of c-Jun expression in regenerating rat retinal ganglion cells. Brain Res. Mol. Brain Res. 30, 61–69.

Ruff, C.A., Staak, N., Patodia, S., Kaswich, M., Rocha-Ferreira, E., Da Costa, C., Brecht, S., Makwana, M., Fontana, X., Hristova, M., Rumajogee, P., Galiano, M., Bohatschek, M., Herdegen, T., Behrens, A., Raivich, G., 2012. Neuronal c-Jun is required for successful

axonal regeneration, but the effects of phosphorylation of its N-terminus are moderate. J. Neurochem. 121, 607–618.
Schaden, H., Stuermer, C.A., Bahr, M., 1994. GAP-43 immunoreactivity and axon regeneration in retinal ganglion cells of the rat. J. Neurobiol. 25, 1570–1578.
Schreyer, D.J., Skene, J.H., 1991. Fate of GAP-43 in ascending spinal axons of DRG neurons after peripheral nerve injury: delayed accumulation and correlation with regenerative potential. J. Neurosci. 11, 3738–3751.
Schwab, M.E., Caroni, P., 1988. Oligodendrocytes and CNS myelin are nonpermissive substrates for neurite growth and fibroblast spreading in vitro. J. Neurosci. 8, 2381–2393.
Smith, P.D., Sun, F., Park, K.K., Cai, B., Wang, C., Kuwako, K., Martinez-Carrasco, I., Connolly, L., He, Z., 2009. SOCS3 deletion promotes optic nerve regeneration *in vivo*. Neuron 64, 617–623.
Smith, R.P., Lerch-Haner, J.K., Pardinas, J.R., Buchser, W.J., Bixby, J.L., Lemmon, V.P., 2011. Transcriptional profiling of intrinsic PNS factors in the postnatal mouse. Mol. Cell. Neurosci. 1, 32–44.
Tan, C.L., Kwok, J.C., Patani, R., Ffrench-Constant, C., Chandran, S., Fawcett, J.W., 2011. Integrin activation promotes axon growth on inhibitory chondroitin sulfate proteoglycans by enhancing integrin signaling. J. Neurosci. 31, 6289–6295.
Tang, W., Ehrlich, I., Wolff, S.B., Michalski, A.M., Wolfl, S., Hasan, M.T., Luthi, A., Sprengel, R., 2009. Faithful expression of multiple proteins via 2A-peptide self-processing: a versatile and reliable method for manipulating brain circuits. J. Neurosci. 29, 8621–8629.
Taymans, J.M., Vandenberghe, L.H., Haute, C.V., Thiry, I., Deroose, C.M., Mortelmans, L., Wilson, J.M., Debyser, Z., Baekelandt, V., 2007. Comparative analysis of adeno-associated viral vector serotypes 1, 2, 5, 7, and 8 in mouse brain. Hum. Gene Ther. 18, 195–206.
Tom, V.J., Steinmetz, M.P., Miller, J.H., Doller, C.M., Silver, J., 2004. Studies on the development and behavior of the dystrophic growth cone, the hallmark of regeneration failure, in an *in vitro* model of the glial scar and after spinal cord injury. J. Neurosci. 24, 6531–6539.
Weber, J.R., Skene, J.H., 1998. The activity of a highly promiscuous AP-1 element can be confined to neurons by a tissue-selective repressive element. J. Neurosci. 18, 5264–5274.